Summary: The study shows that FLUKA MC simulations are effective in modelling of monitoring anatomical changes in patients undergoing CIRT at the Heidelberg Ion-Beam Therapy Center.

European Journal of Medical Physics 125S1 (2024) 104187
doi:10.1016/j.ejmp.2024.104187

PS07.36
MODELING ALANINE DOSE DISTRIBUTION FOR SMALL FIELDS IN FLASH RADIOTHERAPY USING TOPAS

K. Suzart[1], P. Tavares[1], O. Rodrigues, Jr. [1], M. D. P. Potiens[1]

[1]*Nuclear and Energy Research Institute, Radiation Metrology, São Paulo, Brazil*

Introduction: FLASH radiotherapy (FLASH-RT) is a promising approach to cancer treatment, characterized by the delivery of high doses of radiation in a short period of time, within fractions of seconds [1]. In order to demonstrate the FLASH effect, single high doses of radiation delivered in very short times through a limited number of pulses are required.
Materials & Methods: In this work, we will use the TOPAS software to perform dose distribution simulations in small fields. We use electron beams and vary the energies, including 22 MeV with source distances (SSD) of 10 cm and 100 cm. We simulate an alanine with a radius of 2.4 mm and a thickness of 1.5 mm as a material for analysis.
Results: The figure 1 shows the depth dose profiles for 22 MeV electron beam in alanine dosimeter with differences source distances. The results show that with differences in distance from the source, there is no variation in dose distribution.
Summary: The FLASH radiotherapy study has aroused the interest of researchers as it presents promising results in the treatment of cancer. One of the advantages of FLASH radiotherapy is the differential effect between the tumor and healthy tissues [2]. In the present work, we simulate electron beams with 22 MeV energy in small fields, using the FLASH effect. We will use electron beams and vary the energies, including 22 MeV, 60 MeV, 100 MeV and 120 MeV, with source distances (SSD) of 10 cm and 100 cm.
Acknowledgements: Acknowledgments to the funding agencies FAPESP under process number 2017/50332-0, CAPES under process number 88887.704665/2022-0 and CNPq.
Appendix:

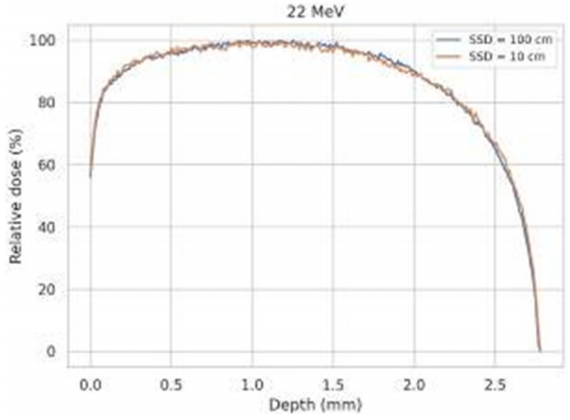

Figure 1: Depth dose profiles for 22 MeV electron beam in alanine dosimeter.

References:

[1] Bourhis J. *et al.* Clinical translation of FLASH radiotherapy: Why and how? *Radiotherapy and Oncology*, v. 139, p. 11–17, 1 out. 2019.
[2] Favaudon V., Caplier L., Monceau V., Pouzoulet F., Sayarath M., Fouillade C., Poupon M.-F., Brito I., Hupé P., Bourhis J., Hall J., Fontaine J.-J., Vozenin M.-C.; "Ultrahigh dose-rate FLASH irradiation increases the differential response between normal and tumor tissue in mice" *Sci Transl Med*, 6, 2014.

European Journal of Medical Physics 125S1 (2024) 104188
doi:10.1016/j.ejmp.2024.104188

PS07.37
ELECTRONIC STOPPING OF PROTONS IN DNA FROM FIRST PRINCIPLES: IMPROVING THE ACCURACY OF DOSE PROFILE AND RANGE

J. José Nogueira Pereira[1], H. Yoriyaz[1], J. Marco Barbosa Shorto[1], P. de Tarso Dalledone Siqueira[1], T. Fiorini da Silva[2], M. Harri Tabacniks[2], N. Koval[3], P. Luis Grande[4], F. Matias[1]

[1]*Instituto de Pesquisas Energéticas e Nucleares - IPEN, São Paulo, Brazil*
[2]*Instituto de Física da Universidade de São Paulo, São Paulo, Brazil*
[3]*Centro de Física de Materiales, Donostia-San Sebastián, Spain*
[4]*Instituto de Física da Universidade Federal do Rio Grande do Sul, Porto Alegre, Brazil*

Introduction: Ions energy-loss in targets, such as DNA, is crucial for understanding radiation effects in cancer therapy [1–3]. The quality of proton radiotherapy planning is directly influenced by accurate information on electronic stopping cross-section (SCS), emphasizing the ongoing importance of its accuracy [4]. This work aims to determine the proton's electronic stopping in DNA using the time-dependent density functional theory (TDDFT) [5–8], combined with the Penn method [9,10], and compare it with the database [11–12]. Furthermore, the dose profile and proton range will be calculated using those electronic stopping TDDFT-Penn results on the MCNP 6.2 code [13].
Materials & Methods: The method for calculating protons' accurate electronic stopping power in realistic materials is based on the TDDFT-Penn approach [5–10]. It uses the energy-loss function (ELF) to weigh the contributions from different electron gas components within a statistical ensemble that characterizes the material of interest [10].
Results: Figure 1, the electronic stopping cross-section (SCS) for protons in DNA is presented: SRIM-2013 (semi-empirical) [14], MELF-GOS (dielectric formalism) [11], results extracted from the MCNP 6.2 code [13], RT-TDDFT [12], and the present results from TDDFT-Penn. The electronic stopping used in MCNP is greatly underestimated in the Bragg peak region. The similarity in the results between SRIM-2013 and MELF-GOS in the Bragg peak suggested that the results from SRIM-2013 are underestimated once the MELF-GOS is a perturbative model.
Summary: TDDFT-Penn has proven to be an excellent tool for generating accurate database results, which are essential in the clinical planning of proton therapy.
Acknowledgements: The authors thank: CAPES (process-88887.704665/2022-00), IPEN (project-2020.06.IPEN.32), CNPq (project-406982/2021-0), FAPESP for supporting the computer cluster (process-2012/04583-8 and 2020/04867-2), and CNPq-INCT-FNA (project-464898/2014-5).
Appendix:

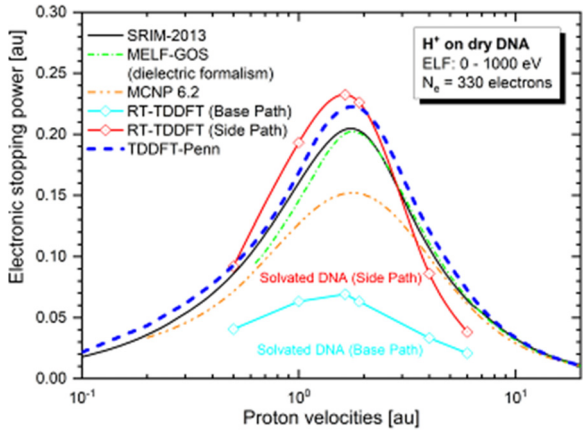

Figure 1: Protons SCS in DNA: SRIM-2013 [13] in a solid line, MELF-GOS [11] in a dash-dot line, and the dash-dot-dot line represents the SCS used in MCNP 6.2 [13]. The symbols are the RT-TDDFT [12]. The short dash line presents the TDDFT-Penn results.

References:

[1] Surdutovich E, Obolensky OI, Scifoni E, Pshenichnov I, Mishustin I, Solov'yov AV., *et al.* Ion-induced electron production in tissue-like media and DNA damage mechanisms. *The European Physical Journal D*. 2009 Jan 31;51(1):63–71.

[2] Solov'yov AV., Surdutovich E, Scifoni E, Mishustin I, Greiner W. Physics of ion beam cancer therapy: A multiscale approach. *Phys Rev E*. 2009 Jan 15;79(1):011909.

[3] Di Pietro C, Piro S, Tabbì G, Ragusa M, Di Pietro V, Zimmitti V, *et al.* Cellular and molecular effects of protons: Apoptosis induction and potential implications for cancer therapy. *Apoptosis*. 2006 Jan 13;11(1):57–66.

[4] Schaffner B, Pedroni E. The precision of proton range calculations in proton radiotherapy treatment planning: experimental verification of the relation between CT-HU and proton stopping power. *Phys Med Biol*. 1998 Jun 1;43(6):1579–92.

[5] Pruneda JM, Sánchez-Portal D, Arnau A, Juaristi JI, Artacho E. Electronic Stopping Power in LiF from First Principles. *Phys Rev Lett*. 2007 Dec 3;99(23):235501.

[6] Quijada M, Borisov AG, Nagy I, Muiño RD, Echenique PM. Time-dependent density-functional calculation of the stopping power for protons and antiprotons in metals. *Phys Rev A (Coll Park)*. 2007 Apr 20;75(4):042902.

[7] Borisov A, Sánchez-Portal D, Díez Muiño R, Echenique PM. Building up the screening below the femtosecond scale. *Chem Phys Lett*. 2004 Mar;387(1–3):95–100.

[8] Quijada M, Díez Muiño R, Borisov AG, Alonso JA, Echenique PM. Lifetime of electronic excitations in metal nanoparticles. *New J Phys*. 2010 May 14;12(5):053023.

[9] Vos M, Grande PL. Extension schemes of the dielectric function, and their implications for ion stopping calculations. *Journal of Physics and Chemistry of Solids*. 2019 Oct;133:187–96.

[10] Matias F, Silva TF, Koval NE, Pereira JJN, Antunes PCG, Siqueira PTD, Tabacniks MH, Yoriyaz H, Shorto JMB, Grande PL. Modeling of Proton Interaction with Organic Polymers: Implications for Cancer Therapy and Beyond, (Manuscript submitted for publication), https://doi.org/10.48550/arXiv.2401.02853.

[11] Abril I, Garcia-Molina R, Denton CD, Kyriakou I, Emfietzoglou D. Energy Loss of Hydrogen- and Helium-Ion Beams in DNA: Calculations Based on a Realistic Energy-Loss Function of the Target. *Radiat Res*. 2011 Feb;175(2):247–55.

[12] Shepard C, Yost DC, Kanai Y. Electronic Excitation Response of DNA to High-Energy Proton Radiation in Water. *Phys Rev Lett*. 2023 Mar 17;130(11):118401.

[13] Goorley T, James M, Booth T, Brown F, Bull J, Cox LJ, *et al.* Features of MCNP6. *Ann Nucl Energy*. 2016 Jan;87:772–83.

[14] Ziegler JF, Ziegler MD, Biersack JP. SRIM – The stopping and range of ions in matter (2010). *Nucl Instrum Methods Phys Res B*. 2010 Jun;268(11–12):1818–23.

European Journal of Medical Physics 125S1 (2024) 104189
doi:10.1016/j.ejmp.2024.104189

PS07.38
ANALYSIS OF A NOVEL QUANTITATIVE CBCT RECONSTRUCTION ALGORITHM: PRELIMINARY RESULTS OF HU VALIDATION IN THE PELVIC REGION

M. C. Daniotti[1,2], S. Trivellato[2], G. Montanari[2], R. M. Niespolo[3], L. de Sanctis[4], V. Pisoni[3], J. Stancanello[5], J. Mason[5], T. Joyce[5], M. Eriksson[5], R. Pellegrini[6], S. Arcangeli[3,4], E. de Ponti[2,4]

[1]*University of Milan, Fisica, Milan, Italy*
[2]*Fondazione IRCCS San Gerardo dei Tintori, Medical Physics Department, Monza, Italy*
[3]*Fondazione IRCCS San Gerardo dei Tintori, Radiation Oncology Department, Monza, Italy*
[4]*University of Milan, School of Medicine and Surgery, Milan, Italy*
[5]*Elekta Intercontinental, Clinical Application Development, Stockholm, Sweden*
[6]*Elekta Intercontinental, Global Medical Affairs, Stockholm, Sweden*

Introduction: A new research platform (Elekta, Sweden) introduces innovative quantitative CBCT (qCBCT) reconstruction algorithms that incorporate scatter correction through a convolutional neural network. Electron densities are provided by Polyquant iterative reconstruction integrating a beam hardening model. This study aimed to conduct preliminary HU validation of qCBCT in the pelvic region for potential use in dose calculation.

Materials & Methods: Raw data from the first fraction-CBCT of two male rectal cancer patients (R1, R2) were used to generate qCBCTs with planning CT voxel-grid. Body contour and OARs were manually segmented in both images. HU median values and ranges were calculated, and distributions compared using Bland-Altman plots. After rigid registration of qCBCT onto CT, a Δimage was produced by subtracting the HU of corresponding voxels, and threshold segmentation was performed within the ranges (-30HU;30HU) and (-50HU;50HU) [1].

Results: Figure 1 presents the statistical outcomes and Bland-Altman plots for R1, as an illustrative example. For both patients, P(CT)-P(CBCT), where P is the percentage of voxel in the considered structure registering a defined HU, was <2% in every structure.

The analysis of Δimages highlighted significant HU discrepancies between CT and qCBCT at the soft tissue-bone interface and within the bowel bag filling, with minor differences in soft tissues.